



Exploiting Global Digital Image Correlation for Crack Initiation

Sylvia Feld-Payet, Vincent Bonnard, Didier Pacou

► To cite this version:

Sylvia Feld-Payet, Vincent Bonnard, Didier Pacou. Exploiting Global Digital Image Correlation for Crack Initiation. *Procedia Structural Integrity*, 2024, 52, pp.517-522. <10.1016/j.prostr.2023.12.051>. <hal-04583332>

HAL Id: hal-04583332

<https://hal.science/hal-04583332v1>

Submitted on 22 May 2024

HAL is a multi-disciplinary open access archive for the deposit and dissemination of scientific research documents, whether they are published or not. The documents may come from teaching and research institutions in France or abroad, or from public or private research centers.

L'archive ouverte pluridisciplinaire **HAL**, est destinée au dépôt et à la diffusion de documents scientifiques de niveau recherche, publiés ou non, émanant des établissements d'enseignement et de recherche français ou étrangers, des laboratoires publics ou privés.



Distributed under a Creative Commons CC BY-NC-ND 4.0 - Attribution - Non-commercial use - No Derivative Works - International License

Fracture, Damage and Structural Health Monitoring

Exploiting Global Digital Image Correlation for Crack Initiation

Sylvia Feld-Payet^{a,*}, Vincent Bonnard^a, Didier Pacou^a^aDMAS, ONERA, Université Paris Saclay, F-92322 Châtillon, France

Abstract

In this work, the authors propose a new methodology to detect automatically crack initiation on the surface of a metallic structure that is initially crack free, independently of the type of material or loading. The proposed strategy relies on the use of a global Digital Image Correlation algorithm based on total variation in order to estimate, first, the moment of gradient localization. This estimation is based on a new criterion that exploits the knowledge of the crack position. Once localization has started, the objective is to be able to detect the smallest possible crack. To do so, the authors propose a new criterion to define a discretized crack from high gradients points and thus be able to estimate its length and orientation. The proposed strategy is applied to nickel based superalloy specimens submitted to low cycle fatigue under biaxial planar loading.

© 2023 The Authors. Published by Elsevier B.V.

This is an open access article under the CC BY-NC-ND license (<https://creativecommons.org/licenses/by-nc-nd/4.0>)

Peer-review under responsibility of Professor Ferri Aliabadi

Keywords: Strain localization; crack initiation; digital image correlation; biaxial fatigue test; mixed mode loading.

1. Introduction

In order to ensure the safety of passenger aircraft, it is necessary to be able to estimate properly the mechanical behavior of the critical parts, especially under cyclic loadings. To do so, models are established from experimental tests that aim at measuring the time before a crack appears or the time before a crack leads to complete ruin. This work focuses on the determination of crack initiation under fatigue loading in metallics. Since there are no reliable means to detect cracks with mode II opening or when plasticity is not confined, the authors propose a new methodology to detect automatically a crack in a structure that is initially crack free, independently of the type of material or loading.

For some aero-engine parts, a crack is usually defined as such if its length is greater than 380 μm in the structure's core or greater than 760 μm on its surface. The proposed methodology must thus at least enable to determine when there is a 760 μm long crack on the surface. In the present case, only surface observations are considered since the proposed analysis relies on digital images.

To exploit these images, maps of maximum gradient of the displacements' norm are considered, following the work of [Feld-Payet et al. \(2020\)](#). In this previous work, the idea was to determine the last not negligible negative

* Corresponding author. Tel.: +33-146-734-565.

E-mail address: sylvia.feld-payet@onera.fr

gradient of the gradient of the maximum gradient standard deviation along the potential crack path, before the plateau. Unfortunately, when studying crack initiation, there is no well-defined crack yet. Consequently, for a given image, it is not possible to exploit data on the crack. However, in a post-processing analysis, it is possible to compare data at the location of the future significant crack (i.e. with a length greater than 760 μm) with data in the surrounding area. This provides a first type of information: the moment of strain localization. Knowledge of the moment of localization is important since it is a sign of loss of integrity, the validity limit of standard continuous models. It could thus be a more conservative crack initiation criterion than the 760 μm one. Once strains are localized, it starts to be possible to approximate the pixels with highly localized gradients with a discrete line. The question is then to determine which part of this line corresponds to a crack and which part corresponds to strains in the continuous medium.

This empirical strategy is applied to nickel based superalloy specimens submitted to low cycle fatigue under biaxial planar loading. In such geometrical configuration presenting a large flat area without stress concentration, crack initiation cannot be easily detected by displacement evolution or the potential drop method.

2. Biaxial fatigue tests' description

2.1. Experimental setup and test conditions

Tests have been performed with a planar biaxial servohydraulic tension-compression fatigue setup. This MTS servohydraulic machine is composed of a rigid frame with 4 cylinders able to deliver $\pm 250\text{kN}$ per axis. A centroid mode enables to maintain the specimen center at a constant location in order to avoid the parasitic bending moments.

The biaxial oligocyclic fatigue tests were performed on cruciform specimens presented in [Selva et al. \(2015\)](#) of dimension $200 \times 200 \times 9.6\text{ mm}$. The initial thickness of the flat cylindrical area, where the cracks initiate, is 1 mm with a finish polish of maximum Ra value of 0.2 μm . The specimens are made of Inconel 718. They are tested at room temperature with an imposed force with a 1 Hz loading frequency. The load ratios are 0.05 for each axis. For the considered test, the biaxiality ratio is $R_b = \frac{F_1^{max}}{F_2^{max}} = 0.4$. Such a test configuration does not allow sufficient detectability of the crack by the electrical potential method or by displacement measurements.

2.2. Optical instrumentation and data acquisition

For image correlation, a speckled pattern is previously obtained by spraying a black paint on a white background, as shown in figure 1. The same methodology is performed on each side of the specimen.

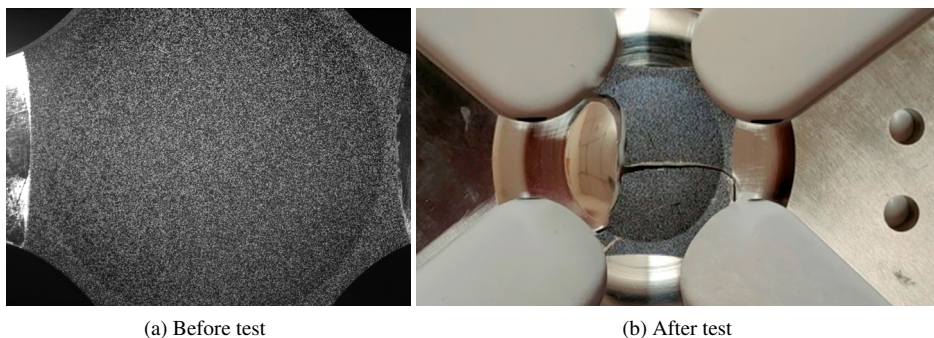


Fig. 1: a: Image of the specimen before the test, used as a reference for digital image correlation. b: Image of the specimen after the test.

The experimental setup is equipped with cameras. On the front side, a stereo-correlation system is used (GOM with 4Mpx cameras), while a PCO camera (2560 \times 2160 px) with a 50 mm fixed focal length lens is dedicated to the rear side. The systems are set to have similar spatial resolutions, i.e. approximately 17.5 μm per pixel (knowing that the grain size for the considered material is approximately 8 μm). The image captures of the two systems are synchronized with the response signal along the main loading axis. They are triggered every 50 cycles. In the present case, the images

taken with the stereo-correlation system enable to attest that the crack appears first on the side observed by the PCO camera. Consequently, only the 207 images of the PCO camera taken at maximum loading are analyzed. Let us note that surface observation is sufficient to analyze crack initiation for the considered test since a fractographic analysis showed that crack initiation took place on the surface.

3. Pre-requisites

3.1. Global digital image correlation exploitation

The proposed strategy relies on strain localization analysis. It is thus important to select an optical flow estimation method that is able to capture the high gradients in the crack area. That is why, following Feld-Payet et al. (2020), the authors choose to use the DeepFlow algorithm proposed by Weinzaepfel et al. (2013). This method rely notably on variational Total Variation-like regularization which makes it possible to obtain both a smooth displacement field far from the crack and highly-resolved high gradients around the crack. This leads to a much better information on the localization of the path and the front of the crack than classical DIC methods based on local window correlation.

From the displacement maps obtained with DeepFlow, the same strain-related scalar field as Feld-Payet et al. (2020) is used to detect strain localization and cracks: the maximum gradients of the displacement norm, g_m (see figure 2). This quantity is simply approximated by finite difference from the displacement norm on adjacent pixels:

$$g_m = \max(\|\mathbf{u}_{i,j+1} - \mathbf{u}_{i,j}\|, \|\mathbf{u}_{i+1,j} - \mathbf{u}_{i,j}\|, \|\mathbf{u}_{i+1,j+1} - \mathbf{u}_{i,j}\|, \|\mathbf{u}_{i-1,j+1} - \mathbf{u}_{i,j}\|) \quad (1)$$

where $\mathbf{u}_{i,j}$ designates the displacement vector for pixel at row i and column j .

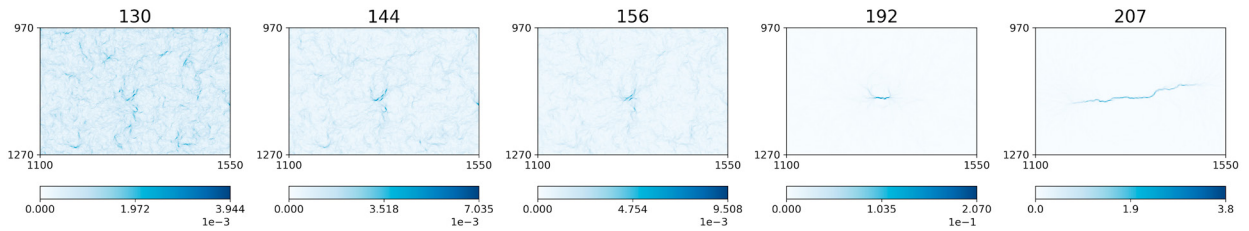


Fig. 2: Maps of the maximum gradients of the displacement norm, g_m , for 5 images: 130, 144, 156, 192 and 207.

3.2. Final crack approximation

The proposed crack initiation determination strategy is meant to be used as a post-processing analysis and can thus take advantage of having at least one image with a significant crack, e.g. the last image of the series (viz. image 207 in the present case, with a crack length exceeding 3 times 760 μm). The corresponding maximum gradient map (shown in figure 2) can then be used to obtain an approximation of the final crack.

To obtain an accurate approximation, it is possible to start by (manually or automatically) determining a coarse linear approximation (in grey in figure 3). Then, a more refined approximation can be obtained by adjusting automatically the row position of the points in each column to the row of maximum gradient (i.e. where the value of g_m is maximum). As the crack path is assumed continuous, the resulting crack estimation is then smoothed thanks to a Savistky-Golay filter (of polynomial degree 3 and window size of 8 pixels). The result can be seen in red in figure 3. Let us underline that, taking into account a refined approximation rather than a straight line is important: indeed, it enables to bring more robustness to the strategy by making it less sensitive to the parameters' choice.

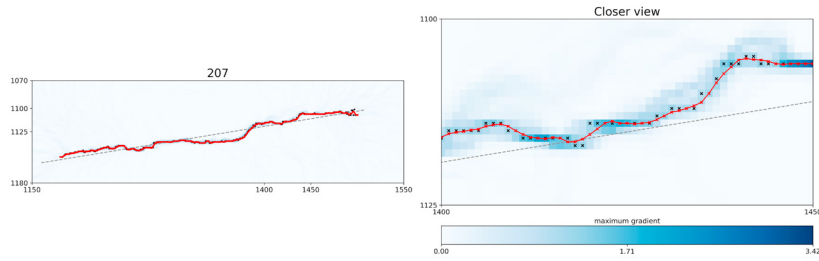


Fig. 3: Maximum gradient map for image 207 with: the coarse linear approximation in grey, the approximation based on the maximum value for each column in black and the filtered crack path estimation in red.

4. Novel developments for crack initiation study

4.1. Strain localization detection

The authors propose to define the moment of strain localization as the moment when the standard deviation of the maximum gradient g_m starts, at some point on the approximation of the final crack, to get significantly larger than the standard deviation in the neighborhood (see figure 4, middle).

From a practical point of view, the evaluation of this standard deviation of the maximum gradient is done, similarly to Feld-Payet et al. (2020), thanks to evaluation windows of 16 pixels large, that are centered at the points of the final crack approximation. Then, the mean value of the 3 points with the highest standard deviation is compared to the standard deviation in the area. This last value is estimated on a grid of evaluation points surrounding the final crack, as depicted in grey in figure 4, left.

Defining the moment where the difference between the standard deviations becomes significant may be challenging because of the noise and the difference's low amplitude. This is why the authors propose to consider that the relative difference is significant when its amplitude gets larger than the noise. In practice, this is done by determining automatically a threshold value: starting at a very low value, the threshold is increased incrementally until the oscillations due to the noise no longer cause the computed difference to cross the threshold. This automatic determination of the threshold is, to the authors' knowledge, an original proposition.

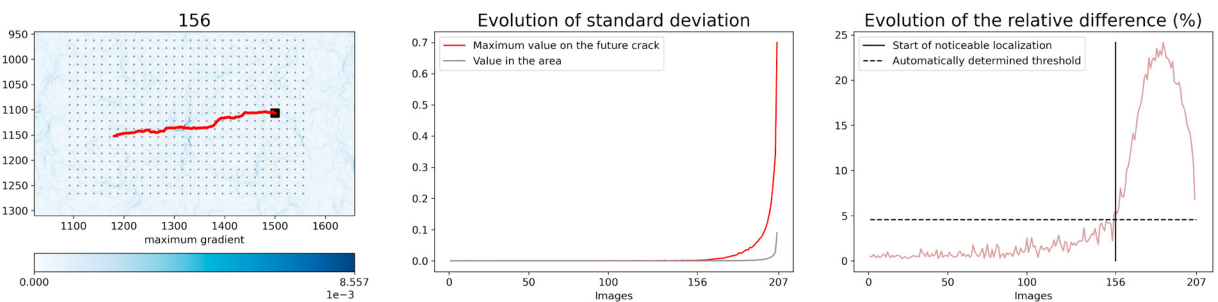


Fig. 4: Left: Maximum gradient map for image 156 with the final crack path for image 207 in red and the grid of points used to evaluate the standard deviation in the area in grey. A moving window used to evaluate the standard deviation is represented in black to better assess its relative size (16 pixels, which is also the step of the evaluation grid). Middle: Evolution of standard deviation on the final crack in red and in the area in grey. Right: Evolution of the relative difference and automatically determined threshold.

For the presented case, the relative difference exceeds the threshold for the first time at image 156 (see figure 4, right). Looking back at the maximum gradient evolution in figure 2, this result seems plausible: indeed, at image 156, there is a region with higher gradients than in the rest of the image. This higher gradients region was present before,

but there were also other regions with a similar level of maximum gradient that could be associated with the measured noise.

Let us note that, if no tolerance for oscillations around the automatically determined threshold is allowed, then the strain localization strategy is very robust and seems to become rather insensitive to the parameters introduced to evaluate the difference. This enables to consider rather large evaluation windows so that less sampling points are needed to cover the studied area, which reduces computational costs. However, if the relative difference signal is allowed to cross the threshold (1 to 3 times maximum), then localization can be detected as soon as image 144 depending on the set of parameters.

4.2. Crack detection

The main difficulty with crack detection is to determine whether a pixel with high gradients corresponds to strain localization or to a true discontinuity. To answer this question, the authors propose to assume that strain localization regions can evolve in time whereas a crack has a constant position and results in a higher gradient. In practice, the authors propose to estimate, for each image after strain localization, a line of highest gradient points. This estimation is done exactly in the same way as described in section 3.2, starting from the coarse linear approximation of the largest crack, but using the maximum gradient map of the considered image to obtain a rather smooth continuous line. Then, for each column, if the point of the highest gradient stays approximately at the same position as the one detected for the final image (i.e. when the crack is much larger), then it is a point of the crack. Given that gradients may be relatively high in a band of a few pixels around the maximum gradient pixel for each column (see figure 2), a row position is considered stable if it is less than 3 pixels away from its estimated final position. These stable points that are assumed to constitute the crack are marked in orange in figure 3. It can be seen that, after strain localization, the stabilized points are divided into 3 groups. These groups can be assumed to be micro-cracks that are going to grow and coalesce until a single crack is formed (as can be seen for the images 156, 160 and 170). The crack then grows in both opposite directions (as can be seen for the images 170, 180, 192 and 195).

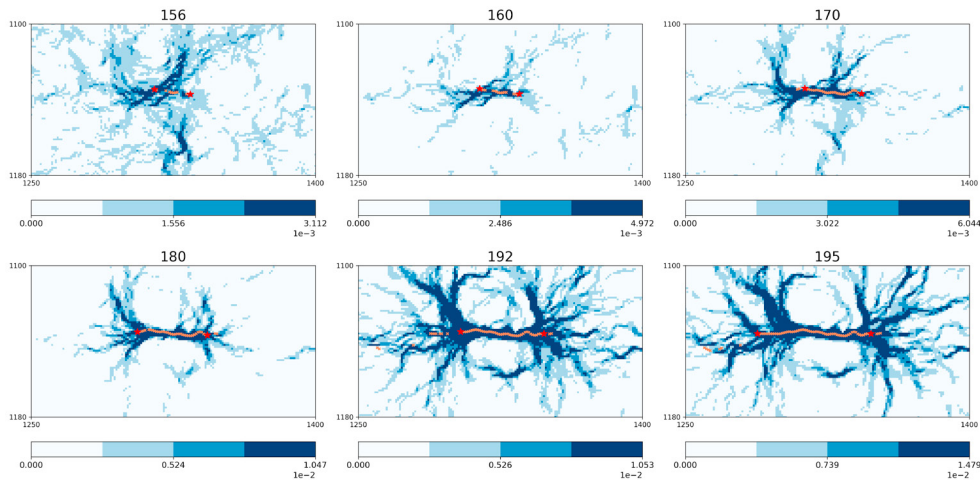


Fig. 5: Maximum gradient map for images 156, 160, 170, 180, 192 and 195 with the stabilized points in orange and the extreme points used for length estimation marked with red stars.

4.3. Crack length evaluation

The next step is to evaluate the crack length to be able to analyze its evolution. The main difficulty is then the lack of continuity. The choice for crack length evaluation then depends on how this piece of information is going to be used. If the goal is to be able to determine for which image a single macrocrack reaches a 760 μm length, then it is sufficient to consider only the distance between the extreme points of the micro-cracks (marked with a red star in

figure 5). Let us note that this is equivalent to consider a linear approximation of the crack, which would correspond to its representation in a finite element computation in the absence of knowledge of the underlying microstructure. However, this approach can only be valid in the coalescence stage where strain localization seems mainly influenced by the microstructure. When a sufficiently long crack is formed, then the strain in the process zone ahead of the crack front may generate high gradients points that stay coincident with the final crack path before the crack appears. In order to not consider the corresponding points, the extreme points are defined with the restriction to have a continuous crack path when the estimated length exceeds $500\text{ }\mu\text{m}$. In practice, this means that there must be a stabilized point in all the columns between the extremities of the crack.

The resulting evolution of estimated crack length is plotted in figure 6, left. Let us notice that the distance between the extreme points is first of the same order of a crack sought in the structure's core in aeronautics (i.e. $335\text{--}380\text{ }\mu\text{m}$). The surface limit of $760\text{ }\mu\text{m}$ is exceeded for the first time on image 192 (see figure 6, right). This point seems to be critical for this test since there is a sudden increase of the crack length between images 191 and 192 (which makes determination of this point less dependent on the parameters involved). Finally, let us note that this length evolution should not be quantitatively exploited for the two last images since image 207 serves as a reference for the stabilized central points but the extremities might still be uncertain.

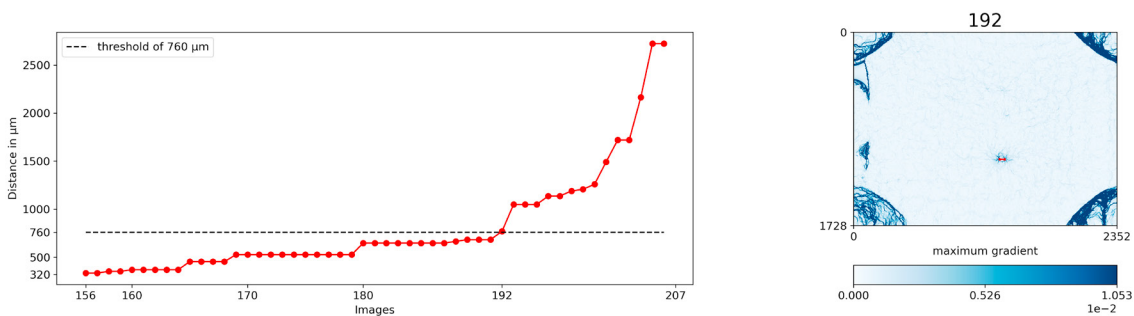


Fig. 6: Left: evolution of the distance between the points marked with a red star. Right: maximum gradient map for image 192 with the corresponding crack in red.

5. Conclusions

A new way to approach crack initiation in a post-processing stage has been proposed in this paper. Taking advantage of the knowledge of the final crack position has enabled to detect the localization moment and to understand the contribution of micro-cracks coalescence in the formation of a single macro-crack. A way to evaluate the crack's geometry and length has been proposed and has led to determine the image where the surface limit of $760\text{ }\mu\text{m}$ has been reached. Future work will focus on applying the proposed methodology on more tests and extending the methodology for in situ control.

Acknowledgements

The authors thank Safran for supporting this study.

References

- Feld-Payet, S., Le Besnerais, G., Bonnard, V., Pacou, D., Thiercelin, L., 2020. Crack path tracking from full field measurements: A novel empirical methodology. , *Strain*, 56, e12333 10.1111/str.12333.
- Selva, P., Lorrain, B., Alexis, J., Seror, A., Longuet, A., 2015. Multiaxial fatigue analysis of a high performance Nickel-based superalloy. *International Journal of Chemical, Molecular, Nuclear, Materials and Metallurgical Engineering* 9, 544–549.
- Weinzaepfel, P., Revaud, J., Harchaoui, Z., Schmid, C., 2013. DeepFlow : Large displacement optical flow with deep matching. *IEEE International Conference on Computer Vision (ICCV)*.